Journal of Power Sources 185 (2008) 1367–1373

Contents lists available at ScienceDirect

Journal of Power Sources

journal homepage: www.elsevier.com/locate/jpowsour

State-of-charge and capacity estimation of lithium-ion battery using a new open-circuit voltage versus state-of-charge☆

Seongjun Lee*, Jonghoon Kim, Jaemoon Lee, B.H. Cho

School of Electrical Engineering and Computer Science, Seoul National University, Seoul 151-744, Republic of Korea

ARTICLE INFO

Article history:
Received 7 May 2008
Received in revised form 21 July 2008
Accepted 28 August 2008
Available online 21 September 2008

Keywords:
State-of-charge
Capacity
Dual extended Kalman filter
Lithium-ion battery

ABSTRACT

Open-circuit voltage (OCV) is widely used to estimate the state-of-charge (SoC) in many SoC estimation algorithms. However, the relationship between the OCV and SoC cannot be exactly same for all batteries. Because the conventional OCV–SoC differs among batteries, there is a problem in that the relationship of the OCV–SoC should be measured to estimate accurately the SoC. Therefore, a modified OCV–SoC relationship based on the conventional OCV–SoC is proposed. Problems resulting from the defects of the extended Kalman filter (EKF) can be avoided by preventing the relationship from varying. Also, in order to improve the performance of the algorithm, measurement noise models of the Kalman filter are applied. Thus, the measurement noise models allow the Kalman filter to overcome defects from the simplified battery modelling and to separate the sequence for estimation of the state and weight filter. The SoC and the capacity of a lithium-ion battery are estimated using the dual EKF with the proposed method.

1. Introduction

The lithium-ion battery is a promising power source for hybrid electric vehicles (HEVs) due to its high specific energy and power. To enable optimum use of the capability of the battery, the HEV requires a battery management system (BMS) [1,2]. An estimation of the state-of-charge (SoC) of the battery should be included in order to prevent the battery from being over or under-charged and to manage the energy flows of the vehicle.

There are several ways to estimate the SoC of a battery [3–5]. The ampere-hour counting method is simple and easy to utilize, but it has problems such as an initial value error and accumulated errors. The open-circuit voltage (OCV) method is very accurate, but it needs a rest time to estimate the SoC and thus cannot be used in real time. To compensate for the shortcomings of these methods, the extended Kalman filter (EKF), which uses the plant model combining the two aforementioned methods, has been presented [4,5]. This method is known to be the optimum adaptive algorithm based on recursive estimation. To improve the performance of the estimation, the model parameters should be chosen correctly. Nevertheless, the parameters of the battery model in the EKF, such as the resistance, capacity and OCV–SoC, are not consistent due to differences in the SoC, temperature and ageing [6,7].

The relationship of the OCV–SoC differs among batteries and therefore the use of this varying OCV–SoC data for the SoC estimation algorithm results in an unacceptable error. In this study, a methodology for defining a new OCV–SoC relationship that is independent of the battery condition is proposed. The capacity, which represents the available energy in the battery, is changed to a new value due to the application of the proposed relationship and a newly defined capacity should be estimated. To achieve this, the dual EKF [5,8] is used to estimate simultaneously the SoC and the capacity.

2. Proposed approach

2.1. Modification of OCV–SoC

The conventional relationship of the OCV–SoC is obtained by measuring the open-circuit voltage at each SoC. The relationship cannot be exactly the same for every battery. The relationship varies with the difference in capacity among batteries and presents different results even if the batteries are fabricated from the same materials and structures, as demonstrated in Fig. 1. Therefore, it is difficult to apply conventional OCV–SoC data to the estimation algorithm. From the viewpoint of the implementation of the algorithm, an equivalent battery model is required, as shown in Fig. 2, and the OCV, as a function of SoC, is utilized as a voltage source. As shown in Fig. 1, the relationship of the OCV–SoC for nine different batteries

☆ The submitted work was presented at the 38th IEEE Power Electronics Specialists Conference (PESC).

* Corresponding author. Tel.: +82 2 880 1785; fax: +82 2 878 1452.
E-mail address: jun2u@pesl.snu.ac.kr (S. Lee).

0378-7753/$ – see front matter © 2008 Elsevier B.V. All rights reserved.
doi:10.1016/j.jpowsour.2008.08.103

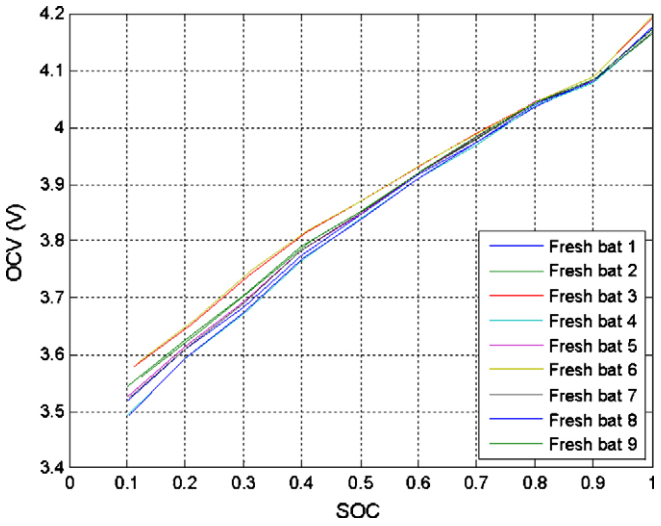

Fig. 1. Conventional OCV–SoC.

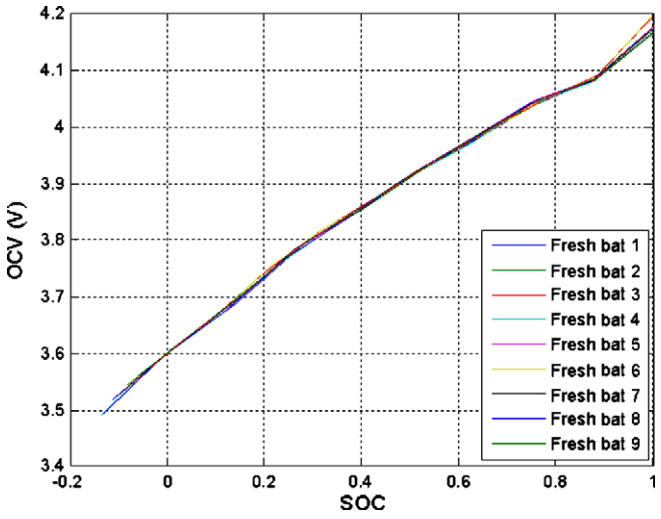

Fig. 3. Proposed OCV–SoC.

is measured under the same conditions. The results exhibit considerable variation, despite the fact that the batteries have almost same capacity. Thus, the use of the varying OCV–SoC relationship among batteries may cause an unacceptable error in the SoC estimation. Measuring the OCV–SoC of each battery for improvement of the estimation performance is a very time-consuming process. Therefore, a new OCV–SoC relationship must be considered.

In this investigation, a new concept of the capacity is defined on the basis of the OCV, and the SoC is modified with respect to the new capacity. To determine the relationship, a cut-off OCV is chosen arbitrarily. In this work, the cut-off voltage is the set voltage, i.e., 3.6 V, as shown in Fig. 3, and the new relationship is configured using the set voltage as a reference voltage. As can be seen in Fig. 3, a strong consistency among the OCV–SoC data of each battery is achieved, regardless of the individual capacities. Thus, a single OCV–SoC can be used for all batteries of the same type. However, the estimation algorithm using the proposed method caused a change in capacity and, therefore, the capacity must be estimated in addition to the SoC.

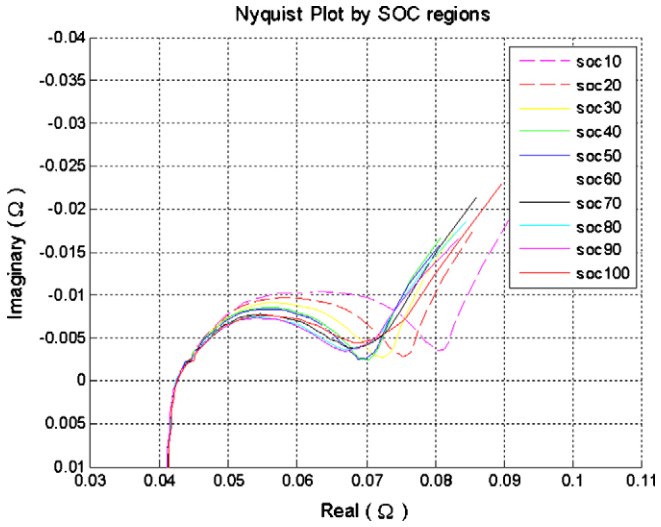

Fig. 4. Nyquist plot measured by EIS.

2.2. Equivalent electrical circuit model

Several researchers have formulated ways to extract the model and its parameters for a battery [9–12]. The modelling approach can generally be classified into two distinctive categories: a frequency domain and a time domain. Impedance measurements of the battery using Nyquist plots, as shown in Fig. 4, are a representative method of the frequency domain analysis. On the other hand, the time domain analysis uses experimental data of the voltage and current of the battery, as shown in Fig. 5.

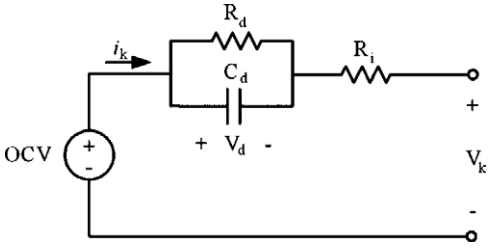

Fig. 2. Simplified battery model.

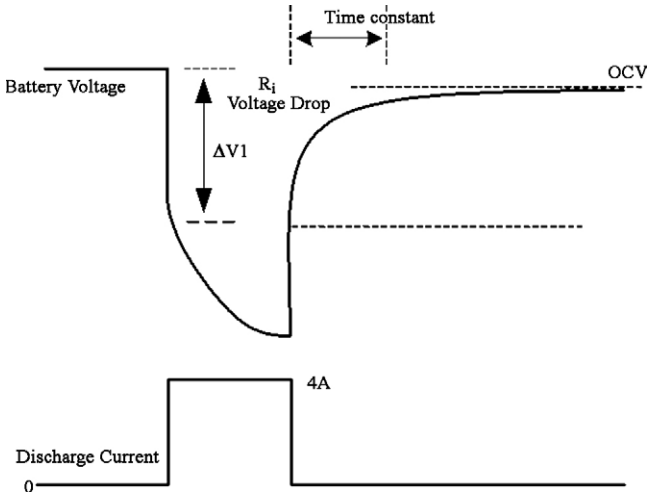

Fig. 5. Voltage response with respect to current reference.

Table 1
Parameters of simplified battery model.

R_i (Ω)	0.041
R_d (Ω)	0.039
C_d (F)	1058

In this study, the current and voltage information of the battery are analyzed to obtain the model and its corresponding parameters. The extracted parameters of the battery through the time domain analysis are similar to those in Fig. 4 and the dynamic behaviour of the battery can be utilized. The resulting simplified battery model is shown in Fig. 2 and the parameters are given in Table 1. First, the OCV, which refers to the equilibrium potential of the battery, is modelled as an equivalent voltage source and is implemented using the proposed relationship. Second, the internal resistance of the battery is modelled as a series resistance R_i. Finally, an RC parallel connection represents the charge transfer, double layer and diffusion.

2.3. Implementation of dual extended Kalman filter

The dual EKF is used to estimate the SoC and capacity of a lithium-ion battery. This algorithm combines the two EKFs, one of which is the state filter, which estimates the SoC, and the other is the weight filter, which estimates the capacity. At every time step, the state filter uses an a priori value of the weight filter, while the weight filter uses an a priori value of the state filter. Therefore, the two EKFs are calculated concurrently to estimate the SoC and capacity. The equations for the state and parameter estimations are given in Table 2.

To improve the performance of the filter, the equivalent model that represents the static and dynamic behaviour of the battery should be well constructed. The equivalent battery model considered in Section 2.2 cannot realistically simulate the non-linear dynamic behaviour of the plant due to the simplified dynamic characteristics [13]. On the other hand, the complicated battery modelling in the simulation of the dynamic behaviour of the battery increases the order of the system, which makes it difficult to implement and operate the estimation algorithm in real time. Thus, the measurement noise model is used to avoid errors between the plant and model [4]. This model can serve to construct the simplified model and prevent the dual EKF algorithm from measurement errors caused by inaccurate modelling.

The state-space representation with difference equations of the dual EKF is described in Eqs. (1)–(3). The symbols w_k^x and w_k^θ represent the process noise of the state filter and weight filter, respectively, are assumed to be independent, zero-mean, Gaussian noise with covariance matrices Q_k^x and Q_k^θ. The measurement noise υ_k is assumed to be independent, zero-mean, Gaussian noise with a covariance matrix R_k. In this work, the state-space equation of the battery model is derived as Eqs. (4)–(6), from the equivalent circuit shown in Fig. 2 and Δt is the time between step k and step $k+1$, which in this case is 0.1 s:

$$x_{k+1} = f_x(x_k, u_k, \theta_k) + w_k^x \tag{1}$$

$$\theta_{k+1} = \theta_k + w_k^\theta \tag{2}$$

$$y_k = h_k(x_k, u_k, \theta_k) + \upsilon_k \tag{3}$$

$$x_{k+1} = \begin{bmatrix} \mathrm{SoC}_{k+1} \\ V_{d,k+1} \end{bmatrix} = \begin{bmatrix} 1 & 0 \\ 0 & 1 - \dfrac{\Delta t}{C_d R_d} \end{bmatrix} \begin{bmatrix} \mathrm{SoC}_k \\ V_{d,k} \end{bmatrix} + \begin{bmatrix} -\dfrac{\Delta t}{C_{n,k}} \\ \dfrac{\Delta t}{C_d} \end{bmatrix} i_k \tag{4}$$

$$\theta_k = [C_{n,k}] \tag{5}$$

$$V_k = \mathrm{OCV}(\mathrm{SoC}_k, C_{n,k}) - V_{d,k} - R_i\ i_k \tag{6}$$

The OCV in the measurement equation is implemented by the proposed relationship of the OCV–SoC data. The measurement matrix is derived from Eqs. (7)–(9). From Eqs. (9)–(11), the measurement matrix of the capacity requires the total differential because the OCV is a function of the SoC. In this case, the first term on the right-hand side of Eq. (9) is irrelevant to the capacity, as shown in Fig. 3, and its value is approximately zero. Hence, the realization of the dual EKF can be simplified.

$$H_k^{\mathrm{SoC}} = \frac{\partial V_t}{\partial \mathrm{SoC}} = \frac{\partial \mathrm{OCV}}{\partial \mathrm{SoC}} \tag{7}$$

$$H_k^{V_d} = \frac{\partial V_t}{\partial V_d} = -1 \tag{8}$$

$$H_k^{C_n} = \frac{d\mathrm{OCV}}{dC_n} = \frac{\partial \mathrm{OCV}}{\partial C_n}\bigg|_{C_n^-} + \frac{\partial \mathrm{OCV}}{\partial \mathrm{SoC}_k^-}\frac{d\mathrm{SoC}_k^-}{dC_n} \tag{9}$$

$$\frac{d\mathrm{SoC}_k^-}{dC_n} = \frac{\partial f(\mathrm{SoC}_{k-1}^+, u_{k-1}, C_n)}{\partial C_n} + \frac{\partial f(\mathrm{SoC}_{k-1}^+, u_{k-1}, C_n)}{\partial \mathrm{SoC}_{k-1}^+}\frac{d\mathrm{SoC}_{k-1}^+}{dC_n} \tag{10}$$

$$\frac{d\mathrm{SoC}_{k-1}^+}{dC_n} = \frac{d\mathrm{SoC}_{k-1}^-}{dC_n} - K_{k-1}\frac{d\mathrm{OCV}^-}{dC_n} \tag{11}$$

Table 2
Dual EKF equations.

Initialization	
$\hat{\theta}_0 = E[\theta], \quad P_{\theta_0} = E[(\theta - \hat{\theta}_0)(\theta - \hat{\theta}_0)^T]$	
$\hat{x}_0 = E[x_0], \quad P_{x_0} = E[(x - \hat{x}_0)(x - \hat{x}_0)^T]$	
Time update	
State filter	$\hat{x}_k^- = f(\hat{x}_{k-1}, u_k, \hat{\theta}_k^-)$ $P_{x_k}^- = F_{k-1}P_{x_{k-1}}F_{k-1}^T + Q^x$
Weight filter	$\hat{\theta}_k^- = \hat{\theta}_{k-1}$ $P_{\theta_k}^- = P_{\theta_{k-1}} + Q^\theta$
Measurement update	
State filter	$K_k^x = P_{x_k}^- H^T (HP_{x_k}^- H^T + R_k)^{-1}$ $\hat{x}_k = \hat{x}_k^- + K_k^x(y_k - H\hat{x}_k^-)$ $P_{x_k} = (I - K_k^x H)P_{x_k}^-$
Weight filter	$K_k^\theta = P_{\theta_k}^-(H_k^\theta)^T[H_k^\theta P_{\theta_k}^-(H_k^\theta)^T + R_k]^{-1}$ $\hat{\theta}_k = \hat{\theta}_k^- + K_k^\theta(y_k - H\hat{x}_k^-)$

3. Control algorithm

As mentioned above, a modelling error occurs due to the simplified battery model. Also, the dual EKF combines the two EKFs and calculates both filters concurrently, which creates difficulties in implementing the filter. Therefore, these problems are overcome by the measurement noise model [4]. In this work, the measurement noise model is extended to separate the state and weight filter, in addition to providing compensation for the model error.

3.1. Measurement noise model for model error

A battery has complicated non-linear dynamic characteristics. Thus, it is modelled as a series resistance, charge transfer, double-layer and diffusion in the impedance-based-model [9]. The diffusion inside the battery can be represented as a Warburg impedance and is equivalent to a chain of RC elements in an electrical circuit. In this study, because the simplified battery model uses one RC parallel circuit, it gives rise to an error voltage in comparison with the plant. Therefore the measurement noise of the EKF is applied at the instant that a large voltage error occurs.

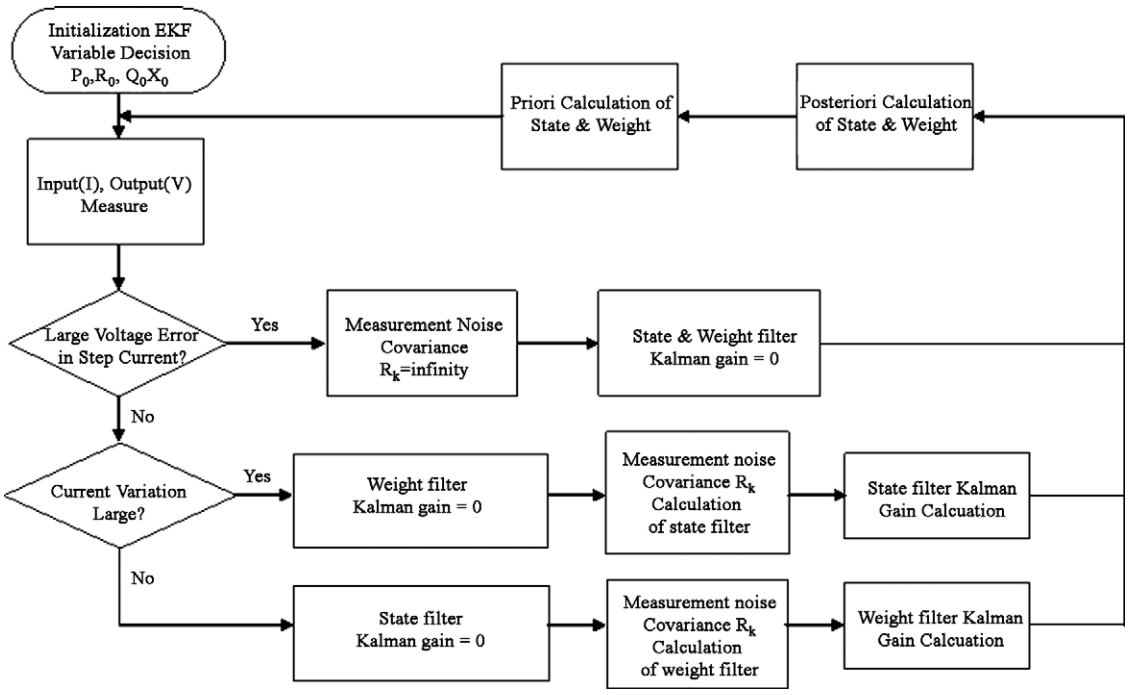

Fig. 6. Algorithm flow chart of dual EKF.

First, if a large voltage error exists in comparison with the plant, during a step current change, the measurement noise model is applied. The measurement noise model is expressed in Eq. (12). The step time denotes the predefined value which decreases from the initial value to zero. In this case, the gain is 0.1 and the initial value of the step time is 100:

$$R_{k+1} = R_k \times (1 + \text{gain} \times \text{step time}) \quad (12)$$

Second, the large voltage error can be increased when the current is large. Because the parameter values differ from those of the plant, the voltage error can increase for a large current. Therefore, the measurement noise model is applied when a large current is imposed. In Eq. (13), the large current denotes a reference set current of 5 A while the gain is defined as 2:

$$R_{k+1} = R_k \times (1 + \text{gain} \times (i_k - \text{large current})) \quad (13)$$

3.2. Measurement noise model for separation of both filters

The dual EKF combines both the state and weight filter. The measurable data is only the terminal voltage of the battery. Thus, it is not easy to estimate the state and parameters at the same time. As a result, the state and weight filters are separated selectively. Because the SoC represents the level of the charge, it is first estimated at initial time. At this time, the estimated capacity is kept to a priori value by setting the measurement noise of the weight filter to a large value. After the set time, which is the initial time required to estimate the SoC, the state and weight filters are used according to the conditions. The non-linear dynamic characteristic of the battery is reduced during the small current variations. Thus, the measurement update of the weight filter is applied. At this time, the measurement noise of the state filter is set to a large value. If the small variation of the current is maintained for a long period of time, the measurement update of the state filter is used

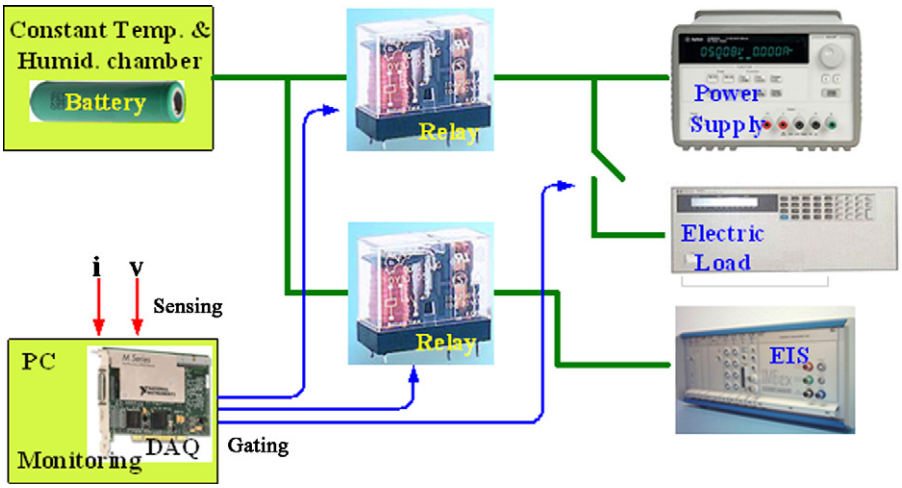

Fig. 7. Experimental set-up.

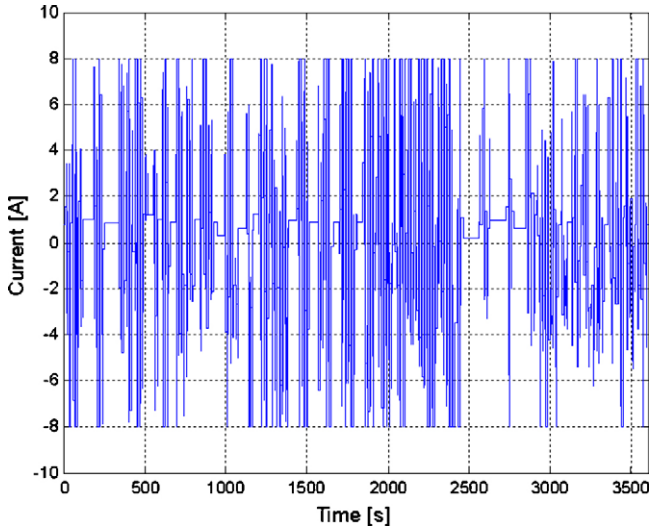

Fig. 8. Current profile.

again to prevent the SoC estimation from facing the disadvantages of ampere-hour counting. The overall control algorithm is shown in Fig. 6.

4. Simulations and experimental results

To verify the proposed OCV–SoC and control algorithms of the dual EKF, simulations and experiments were performed. The experimental equipments was composed of a power supply, an electric load, a constant temperature and humidity chamber, an electrochemical impedance spectroscopy (EIS) instrument, and a personal computer (PC), as shown in Fig. 7. The experimental results from cycling the battery are collected through the data-acquisition board within the PC and are used as an input to the simulations. The Matlab/Simulink S-function is used for the simulations.

The charge–discharge cycling tests of the battery were carried out under the current profile shown in Fig. 8. The lithium-ion batteries used in the experiment are 18650 type with a nominal capacity of 1.3 Ah, i.e., not a typical HEV battery. Thus, the current reference of the HEV automotive driving profile is scaled down to the experimental conditions of Fig. 8. This current profile causes variation of the SoC for one hour and is used to complete a total of eight cycles. Each cycle is different in terms of the number of times the profile is used. The SoC of the battery after completing each cycle is varied from 80 to 40% to verify the estimation results. Verification of the performance of the SoC estimation is achieved through two methods. One is ampere-hour counting and the other is a discharge test. The former is used for the dynamical verification during each cycle and the latter is used for the final verification after completing the cycles. Because the ampere-hour counting method has critical defects, as mentioned above, the battery is fully charged in order to minimize the accumulation error. Thus, because the SoC is reset to the correct value, which represents 100% SoC, before the next cycle, the ampere-hour counting method can be considered to check the general variation trend of the SoC. The estimation of the capacity is verified with the real capacity during all cycles. The real capacity is measured between the fully discharging and charging period between cycles and its values are shown in Fig. 9.

The capacity and SoC measured before cycling are 1.29 Ah and 80%, respectively. Therefore, the estimated SoC and capacity using the proposed methods are changed to the respective conventional

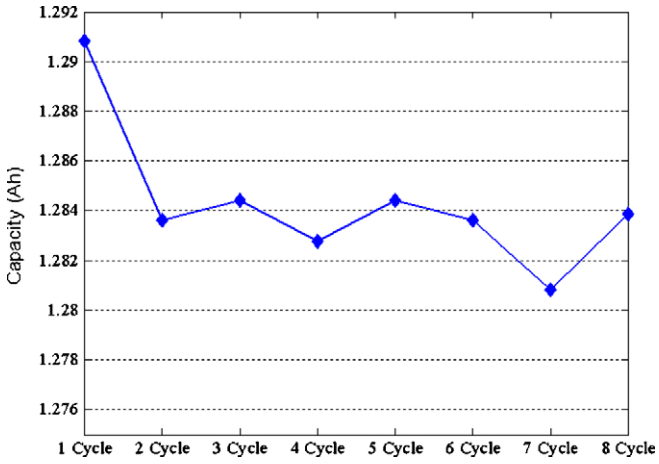

Fig. 9. Capacity variation during cycles.

values, as expressed in Eqs. (14) and (15):

$$\mathrm{SoC} = 1 - (1 - \mathrm{SoC_{new}})(1 - \mathrm{SoC_{cutoff}}) \tag{14}$$

$$\text{conventional capacity} = \frac{\text{modified capacity}}{1 - \mathrm{SoC_{cutoff}}} \tag{15}$$

where $\mathrm{SoC_{new}}$, modified capacity and $\mathrm{SoC_{cutoff}}$ denote the modified SoC, the capacity and the SoC value at the set voltage of the proposed relation of the OCV–SoC, respectively.

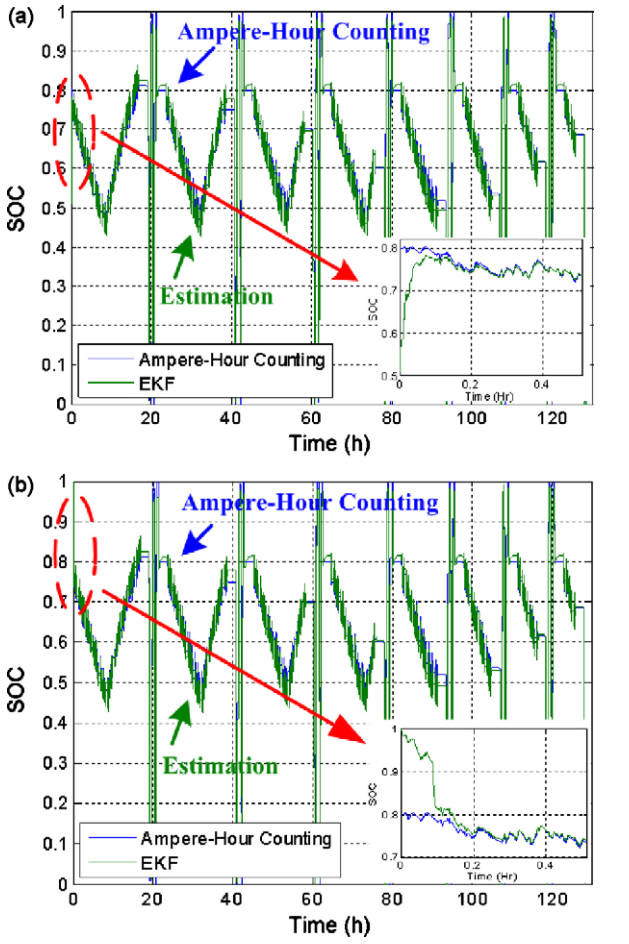

Fig. 10. SoC estimation results of proposed algorithm. (a) SoC estimation with initial error smaller than real value; (b) SoC estimation with initial error larger than real value.

Table 3
SoC estimation results.

	EKF	Discharge test
Cycle 1	0.8164	0.8047
Cycle 2	0.7712	0.7496
Cycle 3	0.7164	0.6819
Cycle 4	0.6259	0.5909
Cycle 5	0.5171	0.4871
Cycle 6	0.5511	0.5345
Cycle 7	0.6282	0.6094
Cycle 8	0.6943	0.6801

The SoC estimation results accurately track the real value within the 60 s in spite of an initial value error, which is smaller than the real value in Fig. 10(a) and larger than the real value in Fig. 10(b). Also, the general trend between ampere-hour counting and the estimated value is almost the same. The performance results through the discharge test after the cycles come within the specifications, specifically within ± 5%, as shown in Table 3. In Fig. 11, the results of the capacity estimation with an initial value smaller than the real value in Fig. 11(a) and larger than the real value in Fig. 11(b) are shown. Both results converge to the real capacity within an error range of 5%. In order to estimate the SoC and capacity simultaneously, the sequence separation of the state and

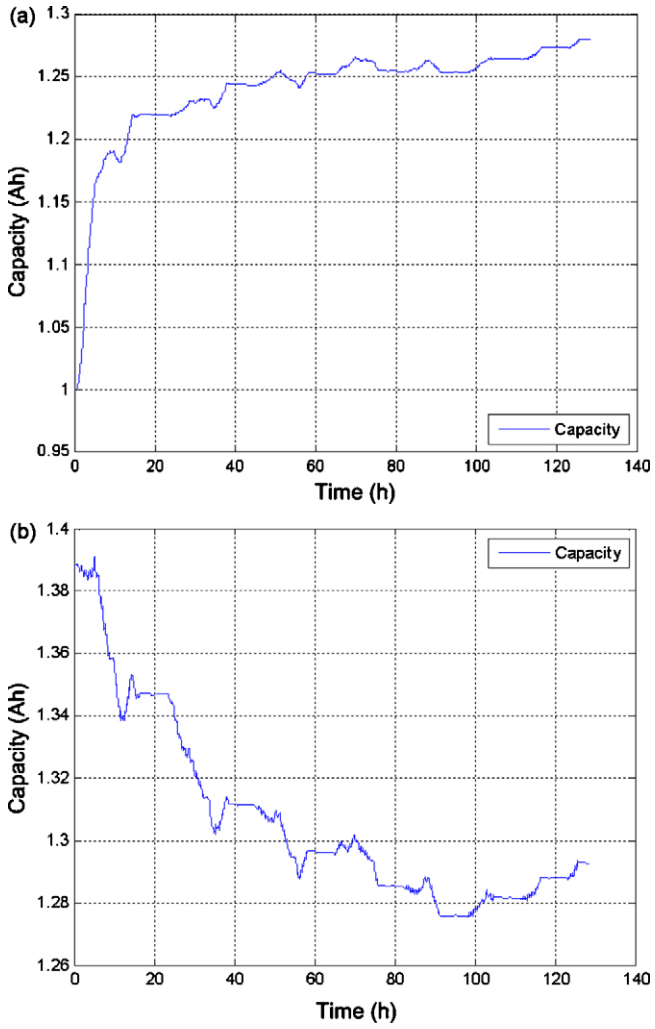

Fig. 11. Capacity estimation results of proposed algorithm. (a) Capacity estimation with initial error smaller than real value; (b) capacity estimation with initial error larger than real value.

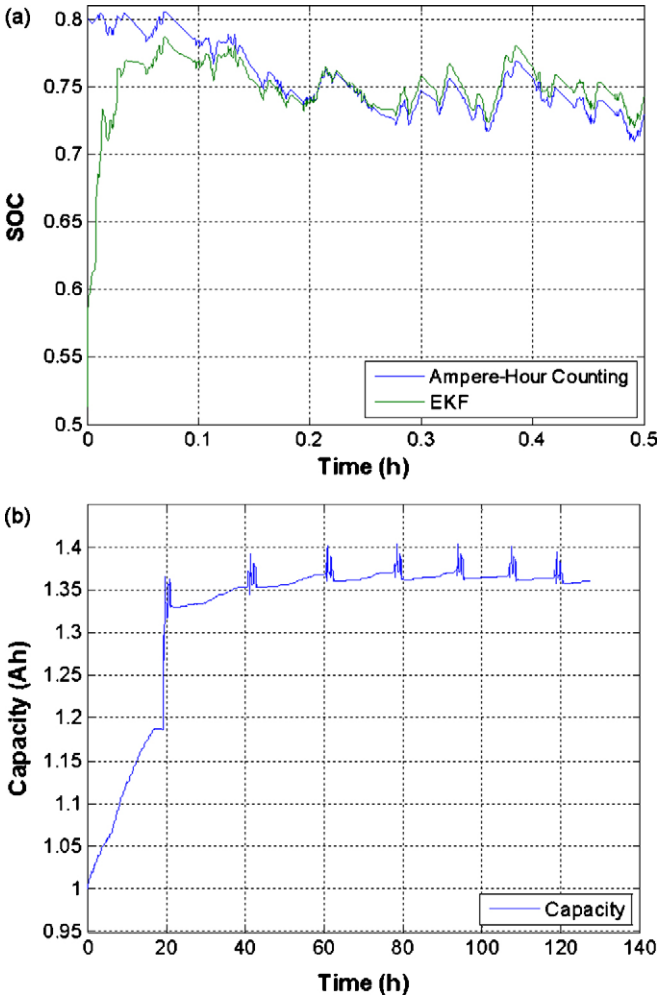

Fig. 12. SoC and capacity estimation results excluded the separation sequence of the proposed method. (a) SoC estimation with initial error smaller than real value, (b) capacity estimation with initial error smaller than real value.

weight filter is used. Although it takes a long time for the convergence by the proposed methods, the accuracy of the estimation is greatly improved. In Fig. 12, the estimation result excluded only the sequence separation under the same condition and shows that the estimation performance cannot be guaranteed by the algorithm. However, the SoC and capacity estimation results of Figs. 10 and 11 represent the validity of the proposed methods.

5. Conclusion

An estimation method using the dual EKF with a modified OCV–SoC is proposed to overcome the variation in conventional OCV–SoC. An explanation of the OCV–SoC relationship and the dual EKF algorithm is given together with experimental results. From the proposed methods, the implementation of the dual EKF can be simplified and the SoC and the capacity can be estimated at the same time. The estimation results of the dual EKF satisfy the specifications within ±5%.

Acknowledgements

This work was supported by the ERC program of MOST/KOSEF (Grant no. R11-2002-102-00000-0) and SAMSUNG SDI.

References

[1] E. Meissner, G. Richter, J. Power Sources 116 (2003) 79.
[2] H.-S. Park, C.-E. Kim, C.-H. Kim, G.-W. Moon, J.-H. Lee, J. Power Electron. 7 (4) (2007) 343–352.
[3] S. Piller, M. Perrin, A. Jossen, J. Power Sources 96 (2001) 113.
[4] J. Lee, O. Nam, B.H. Cho, J. Power Sources 174 (2007) 9–15.
[5] G. Plett, J. Power Sources 134 (2004) 277.
[6] J. Shim, K.A. Striebel, J. Power Sources 122 (2003) 188.
[7] M. Broussely, S. Herreyre, P. Biensan, P. Kasztejna, K. Nechev, R.J. Staniewicz, J. Power Sources 97/98 (2001) 13.
[8] S. Haykin, Kalman Filtering and Neural Networks, Wiley-Interscience, New York, 2001, pp. 123–135.
[9] S. Buller, M. Thele, E. Karden, R.W. De Doncker, J. Power Sources 113 (2003) 422.
[10] S. Abu-Sharkh, J. Power Sources 130 (2004) 266.
[11] S.S. Williamson, S. Chowdary Rimmalapudi, A. Emadi, J. Power Electron. 4 (2) (2004) 117–126.
[12] L. Gao, S. Liu, R.A. Dougal, IEEE Trans. Components Packaging Technol. 25 (3) (2002) 495–505.
[13] A. Jossen, J. Power Sources 154 (2006) 530.